PAPER 16

MEASUREMENT OF INFILTRATION USING FAN PRESSURIZATION AND WEATHER DATA

M. H. SHERMAN AND
D. T. GRIMSRUD

Lawrence Berkeley Laboratory
University of California
USA

Measurement of Infiltration Using Fan Pressurization and Weather Data

M.H. Sherman, D.T. Grimsrud

Energy and Environment Division
Lawrence Berkeley Laboratory
University of California
Berkeley, Ca. 94720

ABSTRACT

In the past expensive instrumentation, usually involving tracer gases, has been required to measure air infiltration; in this paper a technique using fan pressurization results and weather data to calculate infiltration is presented. The geometry, leakage distribution, and terrain and shielding classes are combined into two reduced parameters which allow direct comparison of wind-induced and temperature-induced infiltration. Using these two parameters and the total leakage area of the structure (which is found from fan pressurization) the infiltration can be calculated for any weather condition. Experimental results from fifteen different sites is presented for comparison with theoretical predictions.

INTRODUCTION

Understanding the process of air infiltration is critical to any residential conservation program inasmuchas infiltration is a primary source of energy loss in residences. Yet we are far more capable of calculating conduction losses than losses due to infiltration. The two processes are quite analogous: conduction is the flow of heat due to a temperature difference and infiltration is the flow of air due to a pressure difference. Additionally, to calculate the energy load from air infiltration, the air flow must be combined with the temperature

---

The work described in this report was funded by the Office of Buildings and Community Systems, Assistant Secretary for Conservation and Solar Applications of the U.S. Department of Energy under contract No. W-7405-Eng-48.

difference between inside and outside. Conduction is more easily calculated than infiltration because the heat transfer is proportional to the temperature difference and does not depend strongly on any other driving force. Infiltration, on the other hand, depends on the interior-exterior pressure difference but is not simply proportional to it. Furthermore, the driving pressures are caused by uncorrelated physical effects (wind speed and indoor-outdoor temperature difference). Although conduction losses can be characterized by means of one parameter, the thermal resistance; infiltration, until now, has had no equivalent quantity.

It is because of these problems that infiltration has been a difficult quantity to model. Previous attempts at modeling infiltration have used statistical fitting [1-3] or have involved measurements or calculations that are too difficult to make on a large scale.[4] This paper introduces a model that sacrifices some accuracy for versatility and simplicity. Rather than predicting accurately the weather induced infiltration of a particular structure, the model is designed to calculate the infiltration of a general structure. Furthermore, the model predicts the impact of retrofits or other changes in the building envelope on the basis of performance changes effected in a few measurable parameters.

The parameters used in the model are:

1) The leakage area(s) of the structure.
The leakage area is the parameter that describes the tightness of the structure (obtained by pressurization). Most retrofits will affect the leakage area or the distribution of leakage area around the building envelope (leakage distribution).

2) The height of the structure.
The height and other geometric quantities are usually known or can be measured directly.

3) The inside-outside temperature difference.
The temperature difference gives the magnitude of the stack effect. It is also necessary for calculating the energy load due to infiltration.

4) The wind speed.
The wind speed is required to calculate the wind-induced infiltration for comparison with the stack effect.

5) The terrain class of the structure.

The terrain class of the structure refers to the density of other buildings and obstructions which influence the dependence of wind speed on (measurement) height near the structure. Knowing the terrain class of the structure allows the use of off-site weather data for the calculation of wind-induced pressures.

6) The Shielding

The local shielding determines how much of the wind pressure gets through to the structure.

The wind speed used by the model can be calculated from a wind speed measured on any weather tower in the area. Using standard wind formulas (See Table 1) the wind speed in any terrain class and at any height can be converted to the wind speed at the site. Thus, on-site weather collection is not necessary in our model. We must emphasize, however, that the measured wind data must be for the "same wind", i.e. there can be no mountain ranges or other major terrain obstructions between the site and the wind tower.

AIR LEAKAGE

Air leakage is the simple process of air passing through openings or cracks in the structure. These openings range in size from those of undampered vents (about 0.2m) to tiny cracks around windows (about 0.2mm).

As we know from hydrodynamics, the character of the air flow through a leakage opening changes as the pressure across the opening changes. At very low pressures, the flow is dominated by viscous forces; at high pressures, by inertial forces. Therefore, at low pressures we expect the flow to be proportional to the applied pressure and at high pressures we expect the flow to be proportional to the square-root of the applied pressure. At intermediate pressures the behavior will be a mixture of these effects.

The pressure range in which the flow behavior changes depends on the geometry of the individual crack. While good data[5] exist to describe the functional form of the leakage for an individual crack, the leakage characteristic of the entire structure is much harder to model. The flow vs. pressure curve of the structure will be the summation of all of the curves for each individual crack. Since it is impossible to know the geometry of each crack, calculating the flow vs. pressure curve of a real structure cannot be done from first principles.

Field measurements[6-9] have shown that the behavior of the actual leakage curve more closely resembles that expected for turbulent flow than for viscous flow in the pressure region typical of the pressures that drive infiltration. These findings indicate that the transition pressure (where the flow changes from viscous to turbulent) is below the experimental range. Therefore, in our model, we assume flow to be proportional to the square-root of the applied pressure.

$$Q = A \sqrt{\frac{2}{\rho} \Delta P} \quad (1)$$

where

Q is air flow [m^3/s],

A is the effective leakage area [m^2],

ρ is the density of air [1.2 kg/m^3] and

ΔP is the applied pressure [Pa].

It is the effective leakage area that characterizes the air leakage. In subsequent discussion we will refer to this parameter as the leakage area.

In an actual structure there are many leakage sites, each having a leakage area. In this model we combine the leakage sites into three areas: A_o is the total leakage area of the structure (the sum of the leakage areas of the floor, walls and ceiling), A_f is the leakage area of the floor, and A_c is the leakage area of the ceiling.

As will be shown in the Appendix, it is necessary to differentiate the floor and ceiling leakages from the total leakage area because the stack and wind pressures influence these locations differently.

Leakage Measurement

Air leakage is usually measured by fan pressurization.[4] This technique uses a large-capacity fan to push air either into or out of the structure. Flow continuity requires that all the air that flows through the fan must flow out through the building shell. The graph relating pressure drop across the envelope and the resulting flow is called the leakage curve of the building.

In general, leakage curves obtained by this method will not show a square-root dependence on the pressure drop across the envelope. Our model assumes that there is such a dependency, however, and so we extrapolate the leakage curve (if necessary) down into the pressure range of natural weather effects (0-10 Pa). We then fit the leakage curve to a square-root in that region. The fitting procedure gives us the total leakage area of the structure.

Example: Assume that through fan pressurization tests the following flow vs. pressure data have been measured:

ΔP [Pa]	10	20	30	40	50
Q (m^3/hr]	800	1220	1560	1850	2110

A two-parameter fit of these data to a power law function of the form,

$$Q = C\,\Delta P^{n} \qquad (2)$$

gives us a flow coefficient of 202 and a pressure exponent of 0.6. Thus the data are described by this equation:

$$Q = 202\,\Delta P^{(0.6)}$$

We use this equation to find the flow at our reference pressure. We have chosen 4 Pa as our reference pressure because it is the representative pressure for square-root flow in the 0-10 Pa range.

$$Q(\text{ 4 Pa }) = 464\ \frac{m^3}{hr}$$

Using this 4 Pa flow in Eq. 1, the leakage area is

$$A_o = 500\ cm^2$$

One can estimate the floor and ceiling leakage areas by measurement, by inspection, or by assumption. Direct measurement of the leakage curve for the floor and ceiling is the most accurate method; however, it is difficult and time-consuming. Direct measurement requires isolating the floor and ceiling from the rest of the structure and conducting a separate fan pressurization test. Accordingly, unless very detailed results are desired, direct measurement is usually not warranted.

Unlike walls, floor and ceiling surfaces have few penetrations. Once the penetrations are located and their physical dimensions measured, their leakage areas (usually smaller than the physical area of the opening) can easily be calculated by estimating the discharge coefficient from the geometry of the leaks. Various standard references contain tables or formulae for discharge coefficients. In cases where a floor or ceiling is made of materials that cannot leak (e.g., a slab floor), its leakage area may be assumed to be zero.

Finally, it is possible to assume a value for leakage not accounted for by measurement or calculation. For example, this can be done by assuming that the amount of leakage per unit shell area is the same for all surfaces (i.e. uniform leakage distribution).

INFILTRATION MODEL

In the Appendix we derive a general theory of infiltration. The model is a physical one which makes use of various empirical facts to reduce the complexity. All assumptions made in the derivation are specified in the Appendix.

In this model, we assume that the structure is a single well-mixed zone; we use typical shielding values for a simple rectangular structure and we neglect terms that depend on the sign of the temperature difference. Most importantly, we split the problem into two distinct parts: the wind-regime, where the dynamic wind pressure dominates the infiltration; and the stack-regime, where the temperature difference dominates the infiltration. Infiltration in the two regimes is expressed as follows:

$$Q_{wind} = f_w A_o v \tag{3.1}$$

$$Q_{stack} = f_s A_o \sqrt{gH \frac{\Delta T}{T}} \tag{3.2}$$

where

Q_{wind} is the infiltration in the wind-regime [m^3/s],

Q_{stack} is the infiltration in the stack-regime [m^3/s],

v is the wind speed at ceiling height [m/s],

ΔT is the inside-outside temperature difference [^oK],

g	is the acceleration of gravity [9.8 m/s^2],
H	is the height of the ceiling above grade [m] and
T	is the inside temperature [K].

Derivations for f_w and f_s are presented in the Appendix, but their definitions are

$$f_w = C' (1 - R)^{1/3} \tag{4.1}$$

$$f_s = \frac{1}{3} (1 + R/2) \left[1 - \frac{X^2}{(2 - R)^2} \right]^{3/2} \tag{4.2}$$

C′ is a generalized shielding coefficient; typical values are listed in Table 2 for a variety of local shielding conditions.
R is the fraction of the effective leakage area that is horizontal (i.e. the sum of the floor and ceiling leakage divided by the total leakage).
X is the fractional difference between the floor and ceiling leakage (i.e. the difference in leakage area between the ceiling and the floor divided by the total leakage area):

$$R = \frac{A_c + A_f}{A_o} \tag{5.1}$$

$$X = \frac{A_c - A_f}{A_o} \tag{5.2}$$

The wind speed used in the equations above is the effective wind speed at ceiling height — that is, the wind speed that would exist at the height of the ceiling (above grade) if the building and its immediate surroundings were not there. This wind speed can be calculated from any measurement of the same wind using the following formula:

$$v = v' f_T \tag{6.1}$$

$$f_T = \left[\frac{\alpha \left[\frac{H}{10}\right]^{\gamma}}{\alpha' \left[\frac{H'}{10}\right]^{\gamma'}} \right] \tag{6.2}$$

where

v' is the measured wind speed (e.g. from a weather tower)

f_T is the terrain factor,

H is the height of the ceiling [m],

H' is the height of the wind measurement [m],

α, γ are empirical constants given in Table 1.

The unprimed quantities refer to the structure site and the primed quantities refer to the wind-measurement site.

The expressions for the stack-induced and wind-induced infiltration follow:

$$Q_{stack} = f_s^* A_o \sqrt{\Delta T} \quad (7.1)$$

$$Q_{wind} = f_w^* A_o v' \quad (7.2)$$

where

A_o is the total leakage area [m^2],

f_w^* is the reduced wind parameter,

f_s^* is the reduced stack parameter [$m/s/K^{1/2}$],

ΔT is the inside-outside temperature difference [K] and

v' is the measured wind speed [m/s].

For the definitions of the reduced parameters, see the "Table of Defining Relations" and the "Symbol Table" at the end of the text.

The primary advantage (other than simplicity) of displaying the equations in this form is that it demonstrates the fact that we have separated the weather-independent parts (A_o, f_s^*, f_w^*) from the weather variables (ΔT, v'). Thus the weather-independent parts can be calculated once for a particular structural configuration and combined with weather conditions to predict the infiltration.

Another advantage of this form of the equations is that it demonstrates that the infiltration is proportional to the total leakage area. Hence a fractional change in leakage area corresponds to the same fractional change in infiltration. While it is true that the reduced parameters depend on the relative distribution of the leakage among the floor, walls and ceiling, a small change in the total leakage should not affect them significantly.

Superposition Law for Infiltration

We now have expressions that allow us to calculate the stack-induced infiltration and wind-induced infiltration; the only problem that remains is that of combining them. In general, the interaction of such independent phenomena will be quite complicated but in the spirit of our simplified approach, we look only at the way in which each of them affects the differential pressure. Both the stack effect and wind effect influence the pressure distribution; we assume that their superposition can be treated by simply adding their pressure effects. Since we have assumed a square root dependence of flow on pressure, the stack-induced and wind-induced infiltration add in quadrature.

$$Q = \sqrt{Q_{stack}^2 + Q_{wind}^2} \tag{8}$$

where

Q is the combined infiltration $[m^3/s]$.

In a previous work[13] the authors demonstrated that whenever the wind effect or stack effect dominates, the first order term vanishes, making this type of combinatorial rule possible. Accurate prediction of the infiltration in the intermediate region requires detailed knowledge of both the weather and the structural parameters. On the average, however, the above formula will be correct; we will, therefore, use it for all cases, with the understanding that it is suspect whenever the stack and wind infiltrations are approximately equal.

This way of combining infiltrations can be generalized for any air flow that affects the internal pressure. For example, if there were an exhaust vent in operation, to calculate the total infiltration we would still add the independent air flows in quadrature.

$$Q = \sqrt{Q_{stack}^2 + Q_{wind}^2 + Q_{vent}^2} \qquad (9)$$

where

Q_{vent} is the flow through the exhaust vent [m^3/s].

This superpositional rule does not apply to processes that do not affect the internal pressure, such as the case for a balanced air-to-air heat exchanger that uses both an intake and exhaust fan to push air in and out. There is, indeed, infiltration from this apparatus but because the flows are balanced there is no change in the pressure distribution; therefore, the infiltration caused by the balanced heat exchanger adds simply to the total of the rest of the infiltration.

We can generalize the combination to include balanced and unbalanced flows:

$$Q = \Sigma Q_b + \sqrt{\Sigma Q_u^2} \qquad (10)$$

where

Q_b are the balanced flows [m^3/s] and

Q_u are the unbalanced flows [m^3/s].

In most cases all of the vents in a structure will be exhaust vents and, therefore, their flows can be treated as unbalanced. If, however, there are intake vents as well, that part of the exhaust flow which is balanced by intake flow is balanced flow and the remainder is unbalanced flow.

RESULTS

Fifteen different sites were extracted from the literature to represent a large spread in climate , house construction and measured infiltration rates.[10-12] In all cases, leakage data obtained by fan pressurization were available, permitting us to calculate the effective leakage area. (Note that the effective leakage area varies by a factor of 16 from tightest to loosest.) The fraction of leakage in the floor and ceiling, and the terrain parameters, were estimated from the qualitative description of each site. Table 3 contains summaries of the data extracted for each site.

For most of the sites, the data consist of several short-term infiltration measurements made on a single day. Most infiltration measurements were made using a tracer decay technique[4] averaging infiltration over a one hour period with 5%-10% accuracy. For each measured infiltration point, a predicted infiltration was calculated from the weather variables and house parameters. Figures 1 and 2 contain the plots of predicted vs measured infiltration. Figure 3 displays the deviation of the predicted infiltration (by the percentage difference from the measurement) vs. the leakage area (cm^2) for that site.

DISCUSSION

The separation of the weather-independent from the weather-dependant parts of the model allows the construction of a single graph that can be used to predict the infiltration from the weather data (See Fig. 4) First, the reduced stack and wind parameters are calculated from the geometry, leakage distribution, and terrain and shielding classes. Then these parameters are combined with the weather variables (temperature difference and measured wind speed) to find a point on the graph. This point corresponds to a particular ratio of infiltration to total leakage area as can be read from the curved lines of fig. 4. Finally, the ratio is multiplied by the total leakage area to find the infiltration. Since only the weather variables change over time, this method can be used repeatedly on a single site with a minimum of calculation.

Considering the simplicity of the model and the fact that there are no adjustable parameters*, the agreement is good. However, there are a few sites that do not show particularly good agreement; some overpredict and some underpredict. In order to explain these discrepancies, we examined other factors that may affect the infiltration.

Apparently, the biggest single factor affecting the accuracy of our model is the assumption that directional effects are unimportant. Directional effects could become important if the leakage of the walls varies from wall to wall, or if the shielding varies from face to face — either of which is possible.

---

* We use adjustable to imply that there is no physical meaning associated with that parameter (e.g. regression coefficients). Contrast this with physical parameters that must be estimated (e.g. R).

Aside from directional dependence, non-uniformity of wall leakage area will cause a relative decrease in the actual wind-induced infiltration. For example, if one wall of a structure is much leakier than the rest, it will act like a wind trap; when the wind blows on that wall the internal pressure will rise to mitigate the air flow through that face. Thus the wind-driven infiltration ought to be lower for non-uniform leakage than for uniform leakage. It is generally true that any directional effects will lower the infiltration — on the average.

Most likely, shielding will be the least uniform when it is the greatest, suggesting that directional effects should be more pronounced in more highly shielded situations. If we look at all of the Shielding Class 5 structures (2,8,13) we see a definite pattern of overprediction (19%,43%,19% respectively). While in no way conclusive this may indicate that directional effects are significant for these structures.

Our model has assumed that the floor and ceiling are unaffected by the wind. This assumption is violated whenever a leak through the floor or ceiling leads directly into the wind stream. The most probable instance of this condition is a vent, chimney or flue. If the wind is blowing over the top of a flue the infiltration will be greatly increased over what it would be otherwise. However, this effect is very directional dependent due to the turbulence caused by the wind interacting with the roof structure. The effect will be largest when the flue has a large leakage area; thus we expect to see a large effect in structures that have undampered fireplace chimneys. Two of the test structures had undampered chimneys (10,14) and they showed significant underprediction (-16%,-22% respectively).

While the accuracy of the model is sufficient for a wide variety of applications, the shortcomings described above suggest ways in which accuracy can be improved. Not only can we include new parameters to account for local shielding, but we can extend the model to account for stack flows through vents and flues and for active systems (e.g. furnace fans), all of which may interact with natural ventilation.

Retrofit Evaluation

In addition to predicting the absolute infiltration, the model is useful for predicting the change in infiltration as a result of retrofits. While some retrofits may affect the local shielding, most retrofits that affect infiltration will do so by changing the effective leakage area. Changes in the leakage area affect the three leakage quantities: total leakage area, horizontal fraction, and ceiling/floor difference (A_o, R, and X). For small changes in the total leakage area, the changes in R and X can be ignored and the fractional change in infiltration will be equal to the fractional change in leakage area. If the retrofits affect any of the walls, floor, or ceiling more than another, all three parameters must be used to recalculate the reduced parameters and then the infiltration.

CONCLUSION

We have introduced the concept of leakage area as the characteristic quantity associated with infiltration, just as conductivity is the characteristic quantity associated with conduction. Using this concept, we have devised a model for predicting the infiltration based on a few easily determined physical parameters. Houses of widely different construction types and located in various climatic conditions can be measured and compared by means of this model, inasmuchas all of the parameters used (i.e. leakage areas, terrain classes etc.) have physical reality outside of our model and are, therefore, independently measurable.

In future studies, we will explore long-term average infiltration data from a number of dissimilar sites to test the overall scale of the model. In addition, we will measure infiltration before and after retrofit, comparing the predicted infiltration reduction based on our model with the actual infiltration reduction based on tracer gas measurements.

APPENDIX

Derivation of basic model

In this appendix the basic physical model of infiltration will be derived. The derivation presented in this appendix has been explained in much greater detail in a previous work.[13] Accordingly, we shall present the model used in the text without presenting the useful, though unnecessary, tangents.

First, we separate the driving forces (differential surface pressures) from the response of the structure to the driving forces (air leakage). Second, we combine the surface pressures with the leakage function (and geometry) to calculate infiltration. In the following sections, we will combine these two operations into a complete description of weather-driven infiltration.

<u>LEAKAGE MODEL</u>

Air leakage is the natural flow of air through cracks, holes, etc. across the building envelope. There are two physically well-defined types of air flow: viscous and turbulent. In the viscous regime, the flow is proportional to the applied pressure; in turbulent flow, the flow is proportional to the square-root of the applied pressure. The type of flow is determined by the applied pressure and the geometry of the openings.

Recent evidence[6] indicates that even at low pressures the flow through a structure is dominated by turbulent flow. That is, viscous forces do not appear to dominate the air leakage at typical weather-induced pressures. This statement is expressed by the equation,

$$Q_j = A_j \sqrt{\frac{2}{\rho} \Delta P_j} \qquad \text{(A1)}$$

<u>where</u>

Q_j is the flow through the jth leakage site [m^3/s],

A_j is called the effective leakage area of the jth site [m^2],

ΔP_j is the pressure drop across the jth site [Pa].

This expression relates the pressure drop across a particular leakage site to the flow rate through it. The parameter that describes the leakage is the effective leakage area.

Although every leakage site can be given an effective leakage area, in any real situation it will be practically impossible to measure all of the sites in the envelope individually. We therefore restrict our attention to only three different (lumped) leakage areas: the floor, the walls and the ceiling.

SURFACE PRESSURES

Now that we have a way of relating pressure drops across the envelope to air flow through the envelope, we must be able to calculate the differential surface pressures across the envelope caused by the weather.

Differential pressures on a structure are caused by the stack effect and the wind effect. The stack effect is the height-varying, hydrostatic, indoor-outdoor pressure difference caused by a difference in densities of the two bodies of air, which, in turn, is caused by the difference in temperature of the two bodies of air. The wind effect is an exterior pressure shift caused by a stream of air impinging upon a stationary object.

In our previous work we found that the stack effect and wind effect can be treated independently. Accordingly, we separate the problem into two regimes: the stack-regime (where the wind effect is ignored); and the wind-regime (where the stack effect is ignored).

Stack Effect

The stack pressure is caused by the existence of bodies of air at different temperatures having different densities. From hydrostatic equilibrium we know that the change in pressure with respect to height is proportional to the density.

$$\frac{dP}{dh} = - \rho g \qquad (A2)$$

where

P is the static pressure [Pa],

h is the height [m],

ρ is the density of the air [kg/m^3] and

g is the acceleration of gravity [$9.8\ m/s^2$].

In the case of a structure, the inside and outside bodies of air will usually be of different temperatures; therefore, there will be a differential surface pressure that changes with height:

$$\frac{d\Delta P}{dh} = -\rho g \left(1 - \frac{\rho'}{\rho}\right) \tag{A3}$$

where

ΔP is the differential surface pressure [Pa],

ρ is the density of outside air [$1.2\ kg/m^3$],

ρ' is the density of inside air [kg/m^3],.

Using the ideal gas law, we can replace the density difference factor with a temperature difference factor:

$$\frac{d\Delta P}{dh} = -\rho g \frac{\Delta T}{T} \tag{A4}$$

where

ΔT is the inside-outside temperature difference [K] and

T is the inside temperature [295K].

We can now integrate this expression to find the actual pressure difference:

$$\Delta P = \Delta P_o - \rho g h \frac{\Delta T}{T} \tag{A5}$$

where

ΔP_o is the internal pressure shift[Pa].

The internal pressure shift is fixed by the requirement that for every cubic meter of air that enters, a cubic meter must leave the structure. We can rewrite this expression by making these definitions:

$$P_s = \rho \, g \, H \frac{\Delta T}{T} \qquad (A6.1)$$

$$\Delta P_o = P_s \left(1/2 + \mu \right) \qquad (A6.2)$$

where

P_s is the stack pressure[Pa],

H is the height of the structure [m] and

μ is the normalized neutral level.

The neutral level is the height at which the inside and outside static pressures are equal; μ is equal to the height of the neutral divided by the height of the structure minus one half. Equivalently, μ is the difference between the height of the neutral level and the mid-point of the structure divided by the height of the structure.

Solving for the total pressure difference across the envelope,

$$\Delta P = P_s \left(\mu + 1/2 - \frac{h}{H} \right) \qquad (A7)$$

This expression gives us the differential pressure across the envelope, at every point on it. In order to calculate the air flow through the envelope we must integrate the differential pressures with the air leakage over the entire envelope, making sure to keep track of the infiltration and exfiltration separately.

We are assuming that the floor and ceiling are each at a single height and that their leakage can be considered uniform, thus eliminating the need for integration to calculate the flow through these surfaces. Rewriting the expressions by using the definition that floor is at h=0 and, therefore, the ceiling is at h=H, we get:

$$Q^-_{ceiling} = A_c \sqrt{\frac{2}{\rho} P_s \left(1/2 - \mu \right)} \qquad (A8.1)$$

$$Q^+_{floor} = A_f \sqrt{\frac{2}{\rho} P_s \left(1/2 + \mu \right)} \qquad (A8.2)$$

$$Q^{+}_{ceiling} = Q^{-}_{floor} = 0 \qquad (A8.3)$$

where

A_c is the effective leakage area of the ceiling[m^2] and

A_f is the effective leakage area of the floor[m^2].

The superscripts ± imply infiltration/exfiltration respectively

In stack-dominated flow there is no infiltration through the ceiling nor is there any exfiltration through the floor because of the sign of the pressure difference across them.

We can find the infiltration through the walls by integrating from the floor to the neutral level and the exfiltration by integrating from the neutral level to the ceiling. The results are:

$$Q^{+}_{walls} = A_w \sqrt{\frac{2}{\rho} P_s \left(\tfrac{1}{2} + \mu \right)} \left[\frac{2}{3} \left(\tfrac{1}{2} + \mu \right) \right] \qquad (A9.1)$$

$$Q^{-}_{walls} = A_w \sqrt{\frac{2}{\rho} P_s \left(\tfrac{1}{2} - \mu \right)} \left[\frac{2}{3} \left(\tfrac{1}{2} - \mu \right) \right] \qquad (A9.2)$$

where

A_w is the effective leakage area of the walls [m^2].

If we now make the useful definitions,

$$v_s = \sqrt{\frac{2}{\rho} P_s} \qquad (A10.1)$$

$$A_o = A_w + A_c + A_f \qquad (A10.2)$$

$$R = \frac{A_c + A_f}{A_o} \qquad (A10.3)$$

$$X = \frac{A_c - A_f}{A_o} \qquad (A10.4)$$

where

v_s	is the equivalent stack velocity [m/s],
A_o	is the total (effective] leakage area[m^2],
R	is the fraction of leakage in the floor and ceiling and
X	is the effective leakage distribution parameter.

We can rewrite the expressions for the total stack infiltration and exfiltration:

$$Q^{+}_{stack} = A_o\, v_s \left[\frac{R - X}{2} \sqrt{\frac{1}{2} + \mu} + \frac{2}{3} (1 - R) (1/2 + \mu)^{3/2} \right] \qquad (A11.1)$$

$$Q^{-}_{stack} = A_o\, v_s \left[\frac{R + X}{2} \sqrt{\frac{1}{2} - \mu} + \frac{2}{3} (1 - R) \left(\frac{\text{one}}{\text{two}} - \mu \right)^{3/2} \right] \qquad (A11.2)$$

So far μ has been an undetermined parameter; but, by equating the two expressions above we can find an expression for μ. However, this expression is non-linear and cannot be solved in closed form for μ; therefore, we must solve this equation using approximation methods:

$$\mu = \frac{X}{1 + X^2} \, \frac{1}{2 - R} \qquad (A12)$$

This expression has been verified numerically to vary by no more than a few percent from the exact value.

Any errors in the value of the neutral level will be reflected in the lack of equality between the infiltration and exfiltration. Therefore, the best estimate of the actual infiltration will be the average of these two quantities. As before, the equations are non-linear and approximation techniques must be employed to find the stack infiltration:

$$Q_{stack} = \frac{A_o\, v_s}{3} (1 + R/2) \left[1 - \frac{X^2}{(2 - R)^2} \right]^{3/2} \qquad (A13)$$

Again, this expression is accurate to within a couple of percent. In order to simplify the appearance of this expression, we make the following definitions:

$$f_s = \frac{1}{3} \left(1 + R/2 \right) \left[1 - \frac{X^2}{(2 - R)^2} \right]^{3/2} \qquad (A14.1)$$

$$f_s^* = f_s \sqrt{\frac{gH}{T}} \qquad (A14.2)$$

where

f_s is the stack parameter and

f_s^* is the reduced stack parameter $[m/s/K^{1/2}]$.

Using these definitions yields expressions for the stack-regime infiltration:

$$Q_{stack} = f_s A_o v_s \qquad (A15)$$

$$= f_s^* A_o \sqrt{\Delta T}$$

As a final simplification we may define the reduced stack velocity.

$$v_s^* = f_s v_s = f_s^* \sqrt{\Delta T} \qquad (A16)$$

where

v_s^* is the reduced stack velocity[m/s].

The final simplified expression for the stack-induced infiltration is,

$$Q_{stack} = A_o v_s^* \qquad (A17)$$

In the derivation above we used the leakage distribution parameter, X, to find the height of the neutral level. In some circumstances, the height of the neutral level is measured independently. In this case it is possible to derive an effective leakage distribution parameter (X) from the height of the neutral level.

$$X = \frac{4}{3} \mu \left[1 - R + \frac{1 + R/2}{1 + \sqrt{1 - 4 \mu^2}} \right] \qquad (A18)$$

where

X is the effective leakage distribution parameter and

μ is the measured neutral level shift.

This relationship between X and μ is exact.

Wind Effect

The dynamic pressure caused by wind striking a fixed object called the stagnation pressure is given by,

$$P_{st} = \frac{1}{2} \rho v^2 \qquad \text{(A19)}$$

where

P_{st} is the stagnation pressure and

v is the wind speed.

We define the wind speed, v, to be the wind speed at the ceiling height of the structure, as if the structure and immediate surroundings were not there. Thus, in our definition of wind speed, we are excluding any effects of local environment. However, because of the nature of wind dynamics, the wind speed measured at one height in one type of terrain will not be the same as the wind speed measured at another height or in another type of terrain.

To account for this variability, we use a standard formula[14] to calculate the wind speed at any height and terrain class from the wind speed at any other height and terrain class:

$$v = v_o \alpha \left[\frac{H}{10}\right]^{\gamma} \qquad \text{(A20)}$$

where

v is the actual wind speed

v_o is the wind speed at standard conditions

α, γ are constants that depend on terrain class

To calculate the wind speed at one site from measured data at another site, we first use the above formula to calculate the standard wind speed for the measurement site; then the standard wind speed is used to calculate the wind speed at the desired site. Standard conditions are defined to be a height of 10 m and a terrain of class II. The following formulae are useful in the calculation of the actual wind speed:

$$v = v_o \alpha \left[\frac{H}{10}\right]^{\gamma} \tag{A21.1}$$

$$v' = v_o \alpha' \left[\frac{H'}{10}\right]^{\gamma'} \tag{A21.2}$$

$$v = v' \left[\frac{\alpha \left[\frac{H}{10}\right]^{\gamma}}{\alpha' \left[\frac{H'}{10}\right]^{\gamma'}}\right] \tag{A21.3}$$

In these expressions, the primed quantities are from a wind measurement site. Values for the two terrain class dependent parameters are shown in Table 1.

From the above expression we can define a terrain factor, f_T, that converts measured wind speed into effective wind speed:

$$f_T = \left[\frac{\alpha \left[\frac{H}{10}\right]^{\gamma}}{\alpha' \left[\frac{H'}{10}\right]^{\gamma'}}\right] \tag{A22}$$

We must take into account the effect of local environment on the wind pressures felt by the structure. We do this by introducing shielding coefficients* that convert the stagnation pressure into the actual pressure felt by the exterior of the structure.

Full-scale studies [15] have shown that the pressure distribution on flat faces can be adequately described by using the average pressure on the face. Accordingly, there is one shielding coefficient for every

---

* The term shielding coefficient is equivalent to the more standard term of exterior pressure coefficient; the only difference lies in the interpretation. We use the term shielding coefficient to mean the ratio of the average exterior wind pressure to the stagnation pressure at the ceiling height.

face of the structure:

$$\Delta P_j^e = C_j \; {}^1\!/\!_2 \rho v^2 = C_j \; P_{st} \tag{A23}$$

where

ΔP_j^e is the exterior pressure rise due to the wind and

C_j is the shielding coefficient for the jth face.

The shielding coefficients are functionally dependent on the angle between the incident wind and the orientation of the structure. Since we will eventually average the shielding coefficients over angle, we have suppressed their explicit dependence on angle.

Similar to the stack effect, the wind effect causes an internal pressure shift. As long as the shielding coefficients themselves are not functions of wind speed, the internal pressure shift will be proportional to the stagnation pressure:

$$\Delta P_o = C^o \; {}^1\!/\!_2 \rho v^2 \tag{A24}$$

where

ΔPd is the internal pressure shift[Pa] and

C^o is called the internal shielding coefficient.

From these two equations we can calculate the pressure drop across any of the faces:

$$\Delta P_j = (C_j - C^o) \; {}^1\!/\!_2 \; \rho v^2 \tag{A25}$$

To find the infiltration and exfiltration, we must combine this expression with our leakage function:

$$Q^+_{wind} = \sum_{+} A_j \sqrt{\frac{2}{\rho} (C_j - C^o) P_{st}} \tag{A26.1}$$

$$Q^-_{wind} = \sum_{-} A_j \sqrt{\frac{2}{\rho} (C^o - C_j) P_{st}} \tag{A26.2}$$

The +(-) under the summation sign indicates that the exterior shielding coefficient is larger (smaller) than the interior shielding coefficient.

In most cases the ceiling and floor of a structure are well shielded (i.e. there is usually an attic, basement or slab that protects these horizontal surfaces from direct wind effects). Accordingly, we assume that their shielding coefficients are negligible. Substituting the definition of the stagnation pressure and averaging over angle yields,

$$Q^{+}_{wind} = A_w \, v < \sqrt{C_j - C^o} >_+ \tag{A27.1}$$

$$Q^{-}_{wind} = A_w \, v < \sqrt{C^o - C_j} >_- \tag{A27.2}$$

<u>where</u>

$<...>_+$ indicates an average for $C_j > C^o$ and

$<...>_-$ indicates an average for $C_j < C^o$.

The internal shielding coefficient like the neutral level is fixed by the requirement that the exfiltration must equal the infiltration.

Once the internal shielding coefficient has been determined the wind effect infiltration can be calculated from the average of the two wind flows. We obtain:

$$Q_{wind} = \frac{A_o}{2} v \; (1 - R) < \sqrt{| C_j - C^o |} > \tag{A28}$$

We must now evaluate the shielding coefficients to finish the calculation of the wind effect. In most cases, the shielding coefficients of a structure will not be known; therefore, we propose to use wind tunnel data for a typically shaped structure within a turbulent boundary layer. Such a study was done at Colorado State University by Akins, et. al.[16] They considered a structure that had no local obstructions (i.e. there were no obstacles within several structure heights). For this case we find the following values:

$$C^o = -.21 \tag{A29.1}$$

$$< \sqrt{| C_j - C^o |} > = 0.68 \tag{A29.2}$$

In the preceding analysis we completely neglected the effect of the floor and ceiling leakage. Even though we have assumed that the shielding coefficients for the floor and the ceiling are negligible, the shift of the internal pressure due to the internal pressure coefficient will cause either infiltration or exfiltration in both the floor and the ceiling. This effect can be treated empirically by changing the dependence of the wind effect on R:

$$Q_{wind} = \frac{A_o}{2} v (1 - R)^{2/3} < \sqrt{| C_j - C^o |} > \quad \text{(A30)}$$

The wind tunnel measurements have given us an effective shielding coefficient for the case in which there is no local shielding around the structure; however, in most real cases there will be significant obstruction of the air flow in the immediate vicinity of the structure. Therefore, we will generalize the shielding coefficient to allow for different classes of local shielding. The wind-regime infiltration equation can be rewritten to express this:

$$Q_{wind} = A_o \, v \, C' (1 - R)^{2/3} \quad \text{(A31)}$$

where

C' is the generalized shielding coefficient (cf. Table 2).

We can simplify the appearance of this expression much as we did for the stack expressions by defining some new parameters:

$$f_w = C' (1 - R)^{1/3} \quad \text{(A32.1)}$$

$$f_w^* = f_w \, f_T \quad \text{(A32.2)}$$

where

f_w is the wind parameter and

f_w^* is the reduced wind parameter.

This leads to more concise expressions for the wind effect infiltration:

$$Q_{wind} = f_w \, A_o \, v \quad \text{(A33)}$$

$$= f_w^* \, A_o \, v'$$

<u>where</u>

v is the local wind speed [m/s] and

v' is the wind speed measured on a weather tower [m/s].

We define the reduced wind speed as the product of the wind parameter and the effective wind speed:

$$v^{*} = f_{w} v = f_{w}^{*} v' \tag{A34}$$

<u>where</u>

v^{*} is the reduced wind speed [m/s].

This leads to a simple expression for the wind effect infiltration:

$$Q_{wind} = A_{o} v^{*} \tag{A35}$$

REFERENCES

1. D.R. Bahnfleth, D.T. Moseley, and W.S. Harris, "Measurement of Infiltration in Two Residences," ASHRAE Trans., 63, p. 439-452, (1957).

2. J.B. Dick, and D.A. Thomas, "Ventilation Research in Occupied Houses," J. Inst. Heat. Vent. Eng., 19, p. 306-332, (1951).

3. N. Malik, "Field Studies of Dependence of Air Infiltration on Outside Temperature and Wind," Energy and Buildings, 1, p. 281-292, (1978).

4. D.T. Grimsrud, M.H. Sherman, R.C. Diamond, P.E. Condon, and A.H. Rosenfeld, "Infiltration-Pressurization Correlations: Detailed Measurements on a California House," ASHRAE Trans., 85, Part 1 p. 851-865, (1979). Lawrence Berkeley Laboratory Report LBL-7824 (1978)

5. D.W Etheridge, "Crack Flow Equations and Scale Effect," Building & Environment, 12, p. 181-189, (1977).

6. M.H. Sherman, D.T. Grimsrud, and R.C. Sonderegger, "Low Pressure Leakage Function of a Building," Proc. ASHRAE-DOE Conference on the Thermal Performance of the Exterior Envelopes of Buildings, Orlando, Florida, December 1979. Lawrence Berkeley Laboratory Report LBL-9162 (1979)

7. A.K Blomsterberg, and D.T. Harrje, "Approaches to Evaluation of Air Infiltration Energy Losses in Buildings," ASHRAE Trans, 85, Part 1 p. 797-815, (1979).

8. D.T. Grimsrud, M.H. Sherman, R.C. Diamond, and R.C. Sonderegger, "Air Leakage, Surface Pressures and Infiltration Rates in Houses," Proc. of the Second International CIB Symposium, Copenhagen, Denmark, May 1979, Lawrence Berkeley Laboratory Report LBL-8828 (1979)

9. D.T. Harrje, A.K. Blomsterberg, and A. Persily, "Reduction of Air Infiltration due to Window and Door Retrofits in an Older Home," Princeton University/Center for Environmental Studies Report No. 85, (1979).

10. D.T. Grimsrud, M.H. Sherman, A.K. Blomsterberg, and A.H. Rosenfeld, "Infiltration and Air Leakage Comparisons: Conventional and Energy Efficient Housing Designs," Presented at the International Conference on Energy Use Management, Los Angeles, October 1979. Lawrence Berkeley Laboratory Report LBL-9157 (1979)

11. Johns-Manville Research and Development Center, "Demonstration of Energy Conservation through Reduction of Air Infiltration in Electrically Heated Houses," RP 1351-1, (1979).

12. G.T. Tamura, "The Calculation of House Infiltration Rates," ASHRAE Trans, 85, Part 1 p. 58-71, (1979).

13. M.H. Sherman, D.T. Grimsrud, "Infiltration-Pressurization Correlations: Simplified Physical Modeling," ASHRAE Trans. 86 Part II (1980), Lawrence Berkeley Laboratory Report LBL-10163 (1980)

14. European Convention for Constructional Steelwork, "Recommendations for the Calculation of Wind Effects on Buildings and Structures", Technical General Secretariat, Brussels, Belgium September 1978.

15. S. Kim, K.C. Mehta, "Full Scale Measurements on a Flat Roof Area," Proceedings of the Fifth Int. Conf. Wind Engineering, Boulder, Colorado, July 1979.

16. R.E. Akins, J.A. Peterka, and J.E. Cermak, "Average Pressure Coefficients for Rectangular Buildings," Proceedings of the Fifth Int. Conf. Wind Engineering, Boulder, Colorado, July 1979.

ACKNOWLEDGMENT

The authors would like to thank all the members of the Academy for heir support and guidance in the preparation of this report.

TABLE 1: Terrain Parameters for Standard Terrain Classes			
Class	γ	α	Description
I	0.10	1.30	Ocean or other body of water with at least 5km of unrestricted expanse
II	0.15	1.00	Flat terrain with some isolated obstacles (e.g. buildings or trees well separated from each other
III	0.20	0.85	Rural areas with low buildings, trees, etc.
IV	0.25	0.67	Urban, industrial or forest areas
V	0.35	0.47	Center of large city (e.g. Manhattan)

Table 2: Generalized Shielding Coefficient vs. Local shielding

Shielding Class	C′	Description
I	0.34	No obstructions or local shielding whatsoever
II	0.30	Light local shielding with few obstructions
III	0.25	Moderate local shielding, some obstructions within two house heights
IV	0.19	Heavy shielding, obstructions around most of perimeter
V	0.11	Very heavy shielding, large obstruction surrounding perimeter within two house heights

TABLE 3.1 : Test Results for Test Site #1

Site ID:	IVANHOE
Reference No.	10
House Volume[1]:	480
No. of Stories:	2
Leakage Area[2]:	100
Terrain factor:	.85
Shielding Class:	3
Reduced wind parameter:	.19
Reduced stack parameter[3]:	.16

Predicted and Measured Infiltration[4]				
Stack	Wind	Total Predicted	Measured	Difference
27	27	38	58	-34%
27	55	61	58	5%
27	41	49	48	2%

TABLE 3.2 : Test Results for Test Site #2

Site ID:	Nogal
Reference No.	10
House Volume[1]:	290
No. of Stories:	1
Leakage Area[2]:	960
Terrain factor:	.70
Shielding Class:	5
Reduced wind parameter:	.08
Reduced stack parameter[3]:	.10

Predicted and Measured Infiltration[4]				
Stack	Wind	Total Predicted	Measured	Difference
60	47	76	64	19%

1) m^3 2) cm^2 3) $m/s/K^{1/2}$ 4) m^3/hr

TABLE 3.3 : Test Results for Test Site #3

Site ID:	Telemark
Reference No.	10
House Volume[1]:	480
No. of Stories:	2
Leakage Area[2]:	140
Terrain factor:	.85
Shielding Class:	2
Reduced wind parameter:	.22
Reduced stack parameter[3]:	.12

Predicted and Measured Infiltration[4]				
Stack	Wind	Total Predicted	Measured	Difference
31	53	61	63	-3%
30	42	52	48	8%
30	32	44	38	16%

TABLE 3.4 : Test Results for Test Site #4

Site ID:	Torey Pines
Reference No.	11
House Volume[1]:	233
No. of Stories:	3
Leakage Area[2]:	200
Terrain factor:	.90
Shielding Class:	4
Reduced wind parameter:	.16
Reduced stack parameter[3]:	.14

Predicted and Measured Infiltration[4]				
Stack	Wind	Total Predicted	Measured	Difference
43	81	92	82	12%
44	69	82	72	14%
44	81	92	98	-6%
44	92	102	98	4%
45	92	103	89	16%

1) m^3 2) cm^2 3) $m/s/K^{1/2}$ 4) m^3/hr

TABLE 3.5 : Test Results for Test Site #5

Site ID: R-10
Reference No. 11
House Volume[1]: 233
No. of Stories: 1
Leakage Area[2]: 330
Terrain factor: .85
Shielding Class: 3

Reduced wind parameter: .15
Reduced stack parameter[3]: .09

Predicted and Measured Infiltration[4]				
Stack	Wind	Total Predicted	Measured	Difference
50	80	94	105	-10%

TABLE 3.6 : Test Results for Test Site #6

Site ID: T1
Reference No. 12
House Volume[1]: 337
No. of Stories: 1
Leakage Area[2]: 330
Terrain factor: .77
Shielding Class: 3

Reduced wind parameter: .14
Reduced stack parameter[3]: .10

Predicted and Measured Infiltration[4]				
Stack	Wind	Total Predicted	Measured	Difference
64	23	68	74	-8%
12	45	46	54	-15%
51	67	84	78	8%

1) m^3 2) cm^2 3) $m/s/K^{1/2}$ 4) m^3/hr

TABLE 3.7 : Test Results for Test Site #7

Site ID:	T2
Reference No.	12
House Volume[1]:	433
No. of Stories:	1
Leakage Area[2]:	680
Terrain factor:	.77
Shielding Class:	3
Reduced wind parameter:	.17
Reduced stack parameter[3]:	.11

Predicted and Measured Infiltration[4]				
Stack	Wind	Total Predicted	Measured	Difference
115	112	161	169	-5%
28	29	40	48	-17%
154	196	249	199	25%

TABLE 3.8 : Test Results for Test Site #8

Site ID:	HAVEN
Reference No.	10
House Volume[1]:	230
No. of Stories:	1
Leakage Area[2]:	770
Terrain factor:	.71
Shielding Class:	5
Reduced wind parameter:	.07
Reduced stack parameter[3]:	.10

Predicted and Measured Infiltration[4]				
Stack	Wind	Total Predicted	Measured	Difference
55	39	67	49	37%
92	58	109	71	54%
88	78	117	85	38%

1) m^3 2) cm^2 3) $m/s/K^{1/2}$ 4) m^3/hr

TABLE 3.9 : Test Results for Test Site #9

Site ID: PURDUE
Reference No. 10
House Volume[1]: 240
No. of Stories: 1
Leakage Area[2]: 855
Terrain factor: .62
Shielding Class: 4

Reduced wind parameter: .11
Reduced stack parameter[3]: .11

Predicted and Measured Infiltration[4]				
Stack	Wind	Total Predicted	Measured	Difference
102	67	122	120	2%
102	67	122	125	-2%
102	136	170	154	10%
107	170	200	166	20%

TABLE 3.10: Test Results for Test Site #10

Site ID: NEILSON
Reference No. 10
House Volume[1]: 250
No. of Stories: 1
Leakage Area[2]: 1275
Terrain factor: .62
Shielding Class: 3

Reduced wind parameter: .15
Reduced stack parameter[3]: .12

Predicted and Measured Infiltration[4]				
Stack	Wind	Total Predicted	Measured	Difference
123	138	185	175	6%
135	138	193	160	21%
110	69	130	185	-30%
123	69	141	340	-59%

1) m^3 2) cm^2 3) $m/s/K^{1/2}$ 4) m^3/hr

TABLE 3.11: Test Results for Test Site #11

Site ID:	VALENCIA 1
Reference No.	10
House Volume[1]:	270
No. of Stories:	1
Leakage Area[2]:	560
Terrain factor:	.81
Shielding Class:	3
Reduced wind parameter:	.18
Reduced stack parameter[3]:	.12

Predicted and Measured Infiltration[4]				
Stack	Wind	Total Predicted	Measured	Difference
59	76	96	84	-5%
64	80	102	89	15%

TABLE 3.12: Test Results for Test Site #12

Site ID:	VALENCIA 2
Reference No.	10
House Volume[1]:	270
No. of Stories:	1
Leakage Area[2]:	630
Terrain factor:	.81
Shielding Class:	4
Reduced wind parameter:	.14
Reduced stack parameter[3]:	.12

Predicted and Measured Infiltration[4]				
Stack	Wind	Total Predicted	Measured	Difference
82	143	165	173	14%
61	67	90	78	15%

---

1) m^3 2) cm^2 3) $m/s/K^{1/2}$ 4) m^3/hr

TABLE 3.13: Test Results for Test Site #13

Site ID: FELS
Reference No. 9
House Volume[1]: 470
No. of Stories: 2
Leakage Area[2]: 1480
Terrain factor: .84
Shielding Class: 5

Reduced wind parameter: .08
Reduced stack parameter[3]: .13

Predicted and Measured Infiltration[4]				
Stack	Wind	Total Predicted	Measured	Difference
277	170	325	355	-8%
183	426	464	320	45%

TABLE 3.14: Test Results for Test Site #14

Site ID: SAN CARLOS
Reference No. 10
House Volume[1]: 145
No. of Stories: 1
Leakage Area[2]: 845
Terrain factor: .81
Shielding Class: 4

Reduced wind parameter: .15
Reduced stack parameter[3]: .11

Predicted and Measured Infiltration[4]				
Stack	Wind	Total Predicted	Measured	Difference
0	76	76	149	-49%
47	49	68	116	-41%
47	89	101	90	12%
0	93	93	107	-13%

1) m^3 2) cm^2 3) $m/s/K^{1/2}$ 4) m^3/hr

TABLE 3.15: Test Results for Test Site #15

Site ID:	SOUTHAMPTON
Reference No.	10
House Volume[1]:	1000
No. of Stories:	3
Leakage Area[2]:	1640
Terrain factor:	.90
Shielding Class:	3
Reduced wind parameter:	.20
Reduced stack parameter[3]:	.16

Predicted and Measured Infiltration[4]				
Stack	Wind	Total Predicted	Measured	Difference
94	124	156	250	38%
188	124	255	310	-18%
94	124	156	190	-18%

SYMBOL TABLE	
A	is the effective leakage area [m^2]
A_o	is the total leakage area ($\sum_w A_w + A_f + A_c$)
c	is the subscript indicating the ceiling
C	is a (wind pressure) shielding coefficient
C^o	is the internal (wind) pressure coefficient
C'	is the generalized shielding coefficient
f_s	is the stack-effect factor
f_s^*	is the reduced-stack effect factor [$m/s/\sqrt{^oK}$]
f_T	is the terrain factor
f_w	is the wind-effect factor
f_w^*	is the reduced wind-effect factor
g	is the acceleration of gravity [9.8 m/sec^2]
h	is a height variable [m]

1) m^3 2) cm^2 3) $m/s/K^{1/2}$ 4) m^3/hr

SYMBOL TABLE

H	is the height of the ceiling above grade [m]
H'	is the height of the wind measurement
j	is an index to denote each face of the structure
L	is a semi-empirical constant leakage coefficient
n	is a semi-empirical constant leakage exponent
P_{st}	is the stagnation pressure ($\frac{1}{2}\rho v^2$) [Pa]
P_s	is the stack pressure ($\rho g H \frac{\Delta T}{T}$)
ΔP	is an applied pressure difference.
ΔP_j^w	is the exterior pressure rise due to the wind
ΔP_o	is the internal pressure change
Q	is air flow [m^3/sec]
$Q(\Delta T,v)$	is the instantaneous infiltration
Q_{stack}	is the infiltration in the stack regime
Q_{wind}	is the infiltration in the wind regime
R	fraction of leakage area combined in floor and ceiling
T	is the inside temperature [^oK]
ΔT	is the inside-outside temperature difference
v	is the wind speed at ceiling height [m/sec]
v^*	is the reduced wind speed
v_o	is the wind speed at standard (terrain) conditions
v_s	critical wind speed
v_s^*	reduced critical wind speed
v'	is the measured wind speed
α	is a constant that depends on terrain class (see tables above)
β	is a normalized height
γ	is a constant dependent on terrain class (see tables above)
μ	is the fraction shift in the neutral level from the mid-point
ρ	is the density of air [1.2 kg/m^3]
$\pm$	indicates depressurization/pressurization or infiltration/exfiltration, respectively

Table of Defining Relations

$$R = \frac{A_c + A_f}{A_o}$$

$$X = \frac{A_c - A_f}{A_o}$$

$$f_w = C' \, (1 - R)^{1/3}$$

$$f_s = \frac{1}{3} \, (1 + R/2) \, \left(1 - \frac{X^2}{(2 - R)^2} \right)^{3/2}$$

$$v = v' \, f_T$$

$$f_T = \left[\frac{\alpha \left(\frac{H}{10}\right)^{\gamma}}{\alpha' \left(\frac{H'}{10}\right)^{\gamma'}} \right]$$

$$v^* = f_w \, v = v' \, f_w^*$$

$$f_w^* = f_w \, f_T$$

$$v_s^* = f_s^* \sqrt{\Delta T}$$

$$f_s^* = f_s \sqrt{\frac{gH}{T}}$$

Figure Captions

1) The correlation of infiltration measured using a tracer gas technique and using the model presented in this paper. Dashed lines represent raw measurement error limits. Only data under $150m^3/hr$ is shown.

2) The correlation of infiltration measured using a tracer gas technique and using the model presented in this paper. Dashed lines represent raw measurement error limits. Only data over $100m^3/hr$ is shown.

3) The percentage disagreement between tracer measurements and predictive technique vs leakage area for each site. Solid points are individual measurements; open points with error bars represent site average. Composite for all sites is shown at right.

4) A graphical method for calculating infiltration from weather data. f_s^* and f_w^* are pre-calculated. Combine them with ΔT and v' to find the ratio of infiltration to total leakage area.

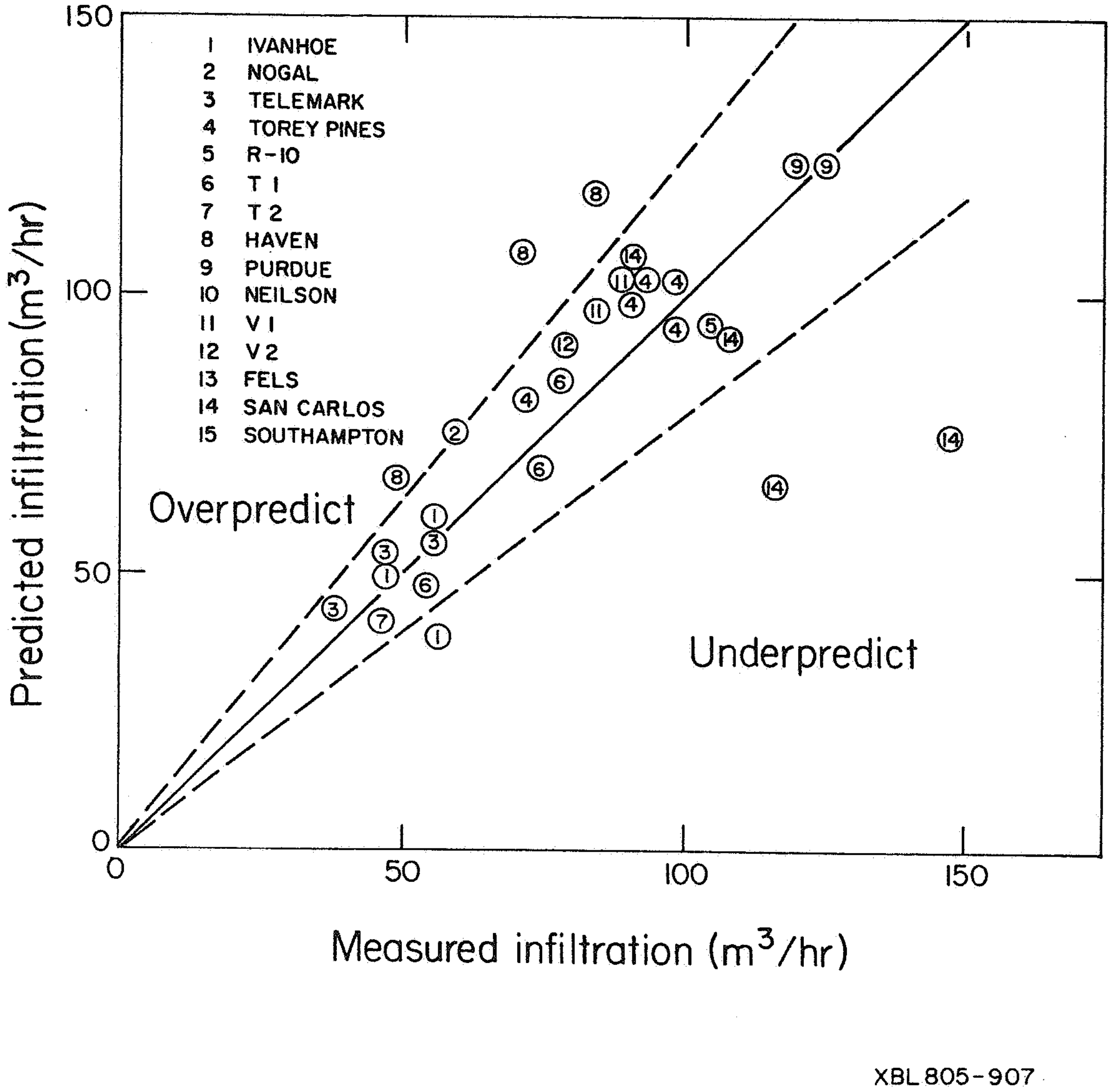
1 IVANHOE
2 NOGAL
3 TELEMARK
4 TOREY PINES
5 R-10
6 T 1
7 T 2
8 HAVEN
9 PURDUE
10 NEILSON
11 V 1
12 V 2
13 FELS
14 SAN CARLOS
15 SOUTHAMPTON
Overpredict
Underpredict
Predicted infiltration (m3/hr)
Measured infiltration (m3/hr)
0
50
100
150
XBL 805-907

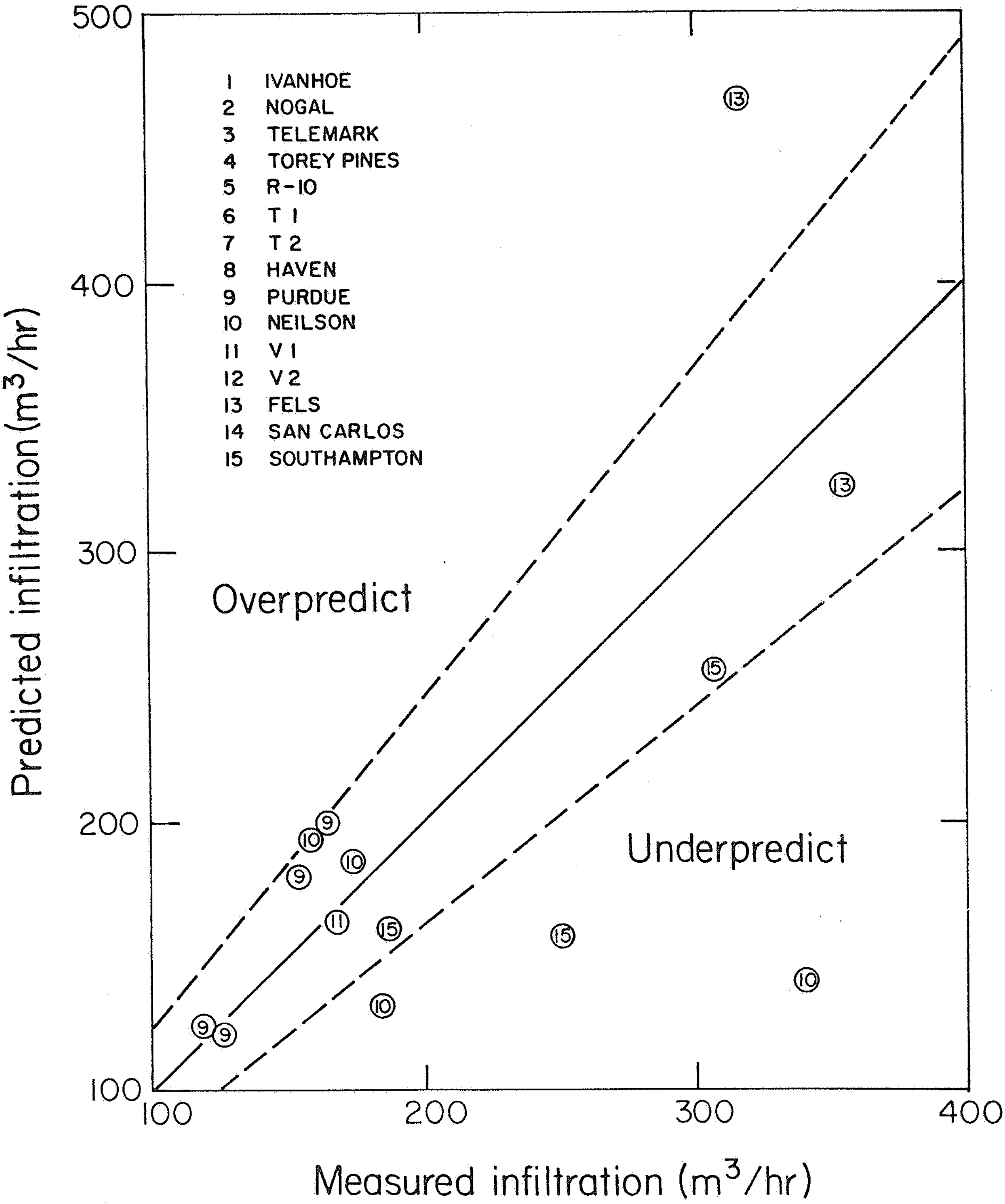
500
400
300
200
100
100
200
300
400
1 IVANHOE
2 NOGAL
3 TELEMARK
4 TOREY PINES
5 R-10
6 T 1
7 T 2
8 HAVEN
9 PURDUE
10 NEILSON
11 V 1
12 V 2
13 FELS
14 SAN CARLOS
15 SOUTHAMPTON
Overpredict
Underpredict
Predicted infiltration (m3/hr)
Measured infiltration (m3/hr)

XBL 805-908

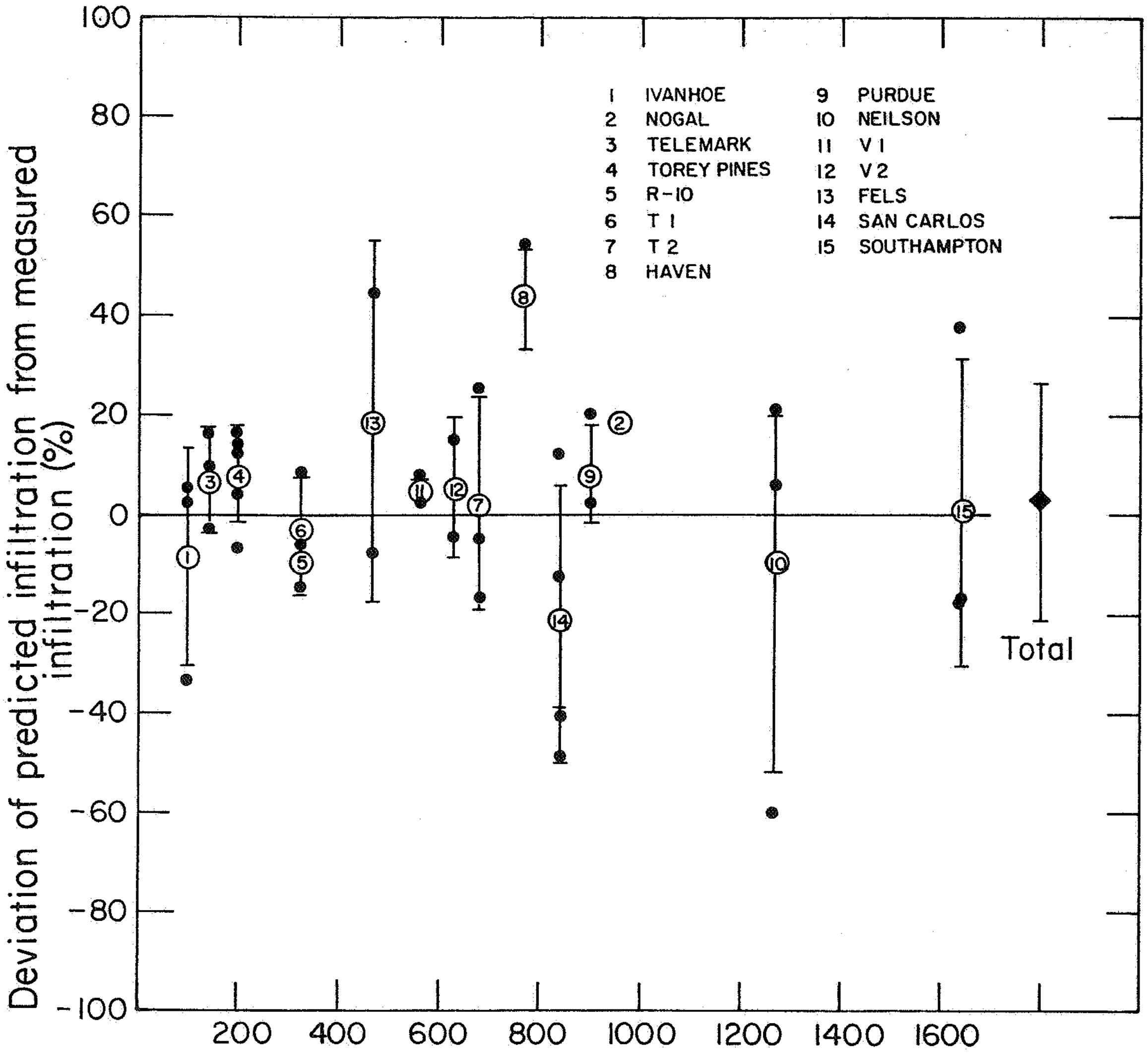

Deviation of predicted infiltration (%) vs leakage area (cm^2)

XBL 805-909

Predicted infiltration per unit leakage area